TECHNICAL MEMORANDUM

126

FGGE re analyses and their use at ECMWF

J. Pailleux, S. Uppala, L. Illari and L. Dell'Osso

Research Department

September 1986

European Centre for Medium-Range Weather Forecasts
Europäisches Zentrum für mittelfristige Wettervorhersage
Centre européen pour les prévisions météorologiques à moyen

E.C.M.W.F.
SCIENTIFIC ADVISORY COMMITTEE
14th SESSION

ECMWF/SAC(86)5
SHINFIELD
17 JULY 1986

Subject: FGGE re-analyses and their use at ECMWF

1. INTRODUCTION

Since the production of the Main FGGE-IIIb analysis, the ECMWF forecasting system has undergone many improvements and the Main FGGE II-b dataset has been enhanced with the collection of other data resulting in a Final FGGE II-b dataset. In view of these developments it was decided to re-analyse part of the Final II-b data using an updated version of the Centre's analysis system.

The periods selected for re-analysis were:

5 December 1978 to 5 March 1979 (includes SOP-I)

5 May 1979 to 31 July 1979 (includes SOP-II)

Prior to carrying out these analyses a considerable amount of preparatory work was carried out in order to improve many aspects of the data assimilation system. As a result many changes were made, of which major ones are:

- improvements to the humidity analysis
- improved treatment of tides in the initialization
- correction of biased cloud-drift winds (SATOBS)

Sections 2 to 5 inclusive of this paper discuss the background to the Centre's re-analysis of the Final FGGE II-b dataset and presents a preliminary assessment of the resulting Final III-b analyses and the impact of these new analyses on forecast skill.

Section 6 of this paper describes recent satellite data experiments carried out using the FGGE data set. The availability of satellite radiance data in the FGGE II-b dataset and the good global data coverage of the TIROS-N and NOAA-6 satellites during November 1979 provides an excellent dataset for the

evaluation of satellite data and retrieval schemes. During 1985 and 1986 an experiment to evaluate one of the University of Wisconsin's "physical retrieval" schemes has been carried out using the Final II-b data for a period in November 1979. The temperature and humidity profiles retrieved in this way have been used to analyse this November period and the resulting analyses have been compared with those based on the Standard (SATEM) retrievals in the FGGE II-b dataset.

2. THE MAIN CHANGES/ADDITIONS IN THE FINAL II-B DATA

The main differences between the Main and Final FGGE II-b datasets can be summarized as follows:

- In the Main dataset only a subset of the conventional data available in WWW was included; in the Final dataset all data has been included which more than doubles the SYNOP data and substantially increases the amount of SHIP data.

- A few additional aircraft reports and TEMPs are included, and mislocated TEMPS have been corrected.

- Additional data from the three monsoon experiments are included.

- US Special Effort SATEMs are available for the SOPs for certain areas.

- US Special Effort SATOBs are included.

- A new set of SATOB winds produced by University of Wisconsin from Japanese HIMAWARI imagery and from Meteosat for 06 and 18 GMT during SOPs are included.

- Additional GOES-Indian Ocean SATOBs are included.

- Reprocessed DROPSONDE and LIMS data are included.

- New quality control information for the drifting buoy data, and Antarctic buoy data (USA) are added.

3. NEW FEATURES IN THE ECMWF DATA ASSIMILATION SYSTEM

The analyses of the Main FGGE II-b data were made with the assimilation system as it was in early 1980. The catalogue of differences between that system and the one for the current re-analyses is a record of the evolution of the assimilation system over the last six years.

Since 1980 the major changes to the assimilation system have been: the interpolation of increments (1980), diabatic initialisation (1982), revised data selection, quality control, structure functions (both horizontal and vertical) (1984), continuous interpolation in the vertical (1984), large scale terms in the correlation functions (1985), use of satellite humidity data, an improved 1-scan humidity analysis, and a correct initialisation of tidal motions (1985/86).

The model used to analyse the Main FGGE II-b data was the original N48 model with the very smooth Berkofski-Bertoni orography. The model used to analyse the Final FGGE II-b data is the T63L16 model (1983), with: mean orography (1983) derived from the high resolution U.S. Navy orography data diurnal cycle (1984), and improved parameterizations (1985/86).

3.1 Analysis changes between Main and Final systems

i) Interpolation of increments (1980)

This modification preserves the structure of the planetary boundary layer in the model and ensures that if data is absent, no change is made to the model. Overall the change reduced spin-up problem and improved the large scale tropical divergence fields.

ii) The 1984 analysis revisions

a) New data selection algorithms and quality control (1984)

With the revised analysis system (Shaw, et al., 1984), the dense Final FGGE II-b data can be utilized by sub-dividing data dense boxes into smaller ones. The 1984 revisions made substantial changes to the quality control algorithms.

b) New optimum-interpolation structure functions (1984)

The major changes have been to introduce a continuous vertical forecast error correlation, instead of empirical discrete correlations, and horizontal correlations expressed as sums of Bessel functions rather than as a Gaussian. The correlation functions have been defined by using operational statistics.

c) Vertical interpolation with continuous functions (1984)

The use of three-dimensionally continuous structure functions provides analysis on model hybrid levels directly from the analysis increments. This has improved boundary layer characteristics during the data-assimilation process.

d) New error statistics

During the Main production rather subjective observational errors were used; they are now more objectively determined. Table 1 shows new and old errors for TEMP wind and height and SATOB winds.

TABLE 1

LEVEL	NEW V SONDE	OLD V SONDE	NEW Z SONDE	OLD Z SONDE	NEW V SATOB
1000	2.20	1.80	5.00	7.00	2.50
850	2.50	1.80	5.40	8.05	2.50
700	2.60	2.50	6.00	8.59	2.50
500	3.10	3.00	9.40	12.07	2.50
400	3.70	3.50	11.60	14.93	5.00
300	3.80	4.00	13.80	18.80	5.00
250	3.30	4.00	14.20	25.38	5.00
200	3.00	4.00	15.20	27.68	5.00
150	2.80	4.00	18.20	32.38	5.00
100	2.40	4.00	21.40	39.35	5.00
70	2.40	4.00	25.20	50.34	5.00
50	2.40	4.00	29.80	59.32	5.00
30	2.50	4.00	31.20	69.80	5.00
20	3.10	4.00	38.10	96.04	5.00
10	3.50	4.00	50.00	114.16	5.00

Units: V m/s; Z m

iii) Large-sale terms in the Mass and Wind correlations (1985)

The correlation functions now include terms which represent height and wind forecast errors on the largest scales representable in the data selection area. These new functions improved the analysis on the largest scales.

iv) Improved humidity analysis (1986)

The humidity analysis scheme available at the time of the Main production was in an early stage of development. In fact the Main FGGE III-b humidity fields are to a very large extent provided by the model first-guess with humidity observations making little impact. Recently, however, the humidity analysis has been reviewed and improved. The structure of the first-guess humidity in the boundary layer has been improved by the parameterization of shallow convection, introduced into the operational model with the revised version of the physics in 1985 (see Tiedtke and Slingo 1985).

The humidity analysis itself has been extensively studied with particular emphasis on the quality of satellite precipitable water content (PWC) data, previously not used (a detailed account can be found in Illari (1985) and Pasch and Illari (1985)). Collocation studies have shown that the radiosonde, satellite and first-guess estimate of precipitable water content are of comparable quality whilst surface information appears of doubtful quality.

Based on these results the following changes to the humidity analysis were implemented:

1) PWC data from satellite is now exploited

2) the use of surface reports has been modified
WW (actual weather) are now not used
cloud cover used to produce bogus humidity data only when the cloud cover is more than 7 oktas

3) a selection procedure for Synops has been introduced: humidity information from Synops are used only when there are no radiosonde data within an analysis box.

Data assimilation experiments have shown that the above changes have a beneficial impact on the moisture analysis particularly in the Tropics. Fig.1 shows the rms and bias of first-guess, analysis and initialised fields, with respect to radiosondes, in the Tropical band (20°N, 20°S) for the CONTROL and NEW HUM experiments, respectively.

It is clear that the rms have been reduced especially above 700 mb, while the bias has been markedly reduced in the 850/700 mb layer, correcting a typical error in the first-guess, which tended to be too moist at the top of the boundary layer.

The impact of changes in the moisture analysis has also been assessed in several forecasts experiments. They generally show improved scores and improved rainfall forecast. In particular, a case study of a Monsoon forecasts has shown that the modified humidity analysis has a beneficial impact on the representation of the Monsoon flow and the forecast of rain (see Fig.2).

3.2 Initialisation changes between Main and Final systems

i) Diabatic non-linear normal mode initialization (1982)

For the Main production an adiabatic version of the non-linear normal mode initialization scheme was used. This had the effect of severely damping the tropical convergence and divergence patterns. With the inclusion of a smoothed representation of diabatic forcing in the initialization, a much larger proportion of the analysed tropical divergence/convergence fields are retained in the analyses (Wergen, 1982).

ii) Tidal initialisation (1986)

Another important modification of the normal mode initialisation concerns the diurnal and semi-diurnal waves of the tides. A realistic propagation of the tides is now allowed in the initialisation scheme (see ECMWF/SAC(86)1 for details).

3.3 Changes in the use of data between Main and Final systems

i) Introduction of a blacklist

During re-assimilation for December 1978 with a preliminary version of the Final system, statistics on the performance of the assimilation scheme were collected. A careful evaluation revealed consistently biased observations, mainly TEMP heights, which were subsequently blacklisted and omitted "marked erroneous", from the analysis.

ii) Treatment of SATOB winds in the analysis

SATOB wind reports are generally underestimates of wind strength especially near jet cores. Kållberg (1985) has derived a method to calibrate SATOB data using as "truth" the colocated aircraft and TEMP/PILOT winds. Uncalibrated GOES-W/NESS and GOES-E/NESS SATOB winds are used north of 20N, all other satellites being excluded. Calibration is performed on all SATOB winds south of 20S (except the GOES). The data are used without any modification between 20S and 20N.

iii) Land surface winds (1984)

Land surface winds have been discarded since the 1984 revisions. This practice is continued in the system for the "Final" system.

iv) Quality control of TOVS data

Sea surface temperature has been used by NESDIS since 1982 to quality control TOVS data where the cloud-clearing algorithm has failed to detect low level cloud. An equivalent modification is made to the quality control of the TOVS data in FGGE.

3.4 Changes in the model between the Main and Final Systems

i) Spectral (T63) forecast model

The Centre's operational T63 spectral model is used in the assimilation, rather than the N48 gridpoint model used for the Main analyses. It has 16 levels in the vertical. The use of a spectral model reduces phase error of small scale features and provides a better first guess.

ii) Improved physical parameterization

The ECMWF model has undergone many changes in the parameterization of physical processes - the inclusion of a diurnal cycle, a revised scheme for shallow convection which improves the humidity structure of the boundary layer, and a new radiation scheme and cloud coverage algorithm.

3.5 Changes in boundary conditions between Main and Final systems

i) Orography (1981)

The main assimilation used the very smooth Berkofski-Bertoni orography. For the re-analysis it was decided to use the mean orography, derived from the high resolution U.S. Navy data.

ii) Analysed sea surface temperature

In the Main production, climatological monthly mean fields of sea surface temperature (SST) were used. For the re-analysis the ECMWF analyses of FGGE SST data are used. These analyses are based on ship and buoy data only; the satellite derived SST in the Main FGGE II-b data had large systematic errors.

4. EVALUATION OF THE FINAL FGGE ANALYSIS

The differences between the GFDL and ECMWF analyses of the Main FGGE II-b dataset gave rise to considerable research to understand the reasons for them. The different intensities of the analysed tropical divergent winds were rapidly traced to the adiabatic normal mode initialisation used in the ECMWF system. The stronger northern hemisphere jets in the ECMWF analyses arose because of the greater weight given to aircraft over cloud-wind reports in the ECMWF system. Many local differences could be traced to differences in quality control, with the ECMWF system generally performing better. In the southern hemisphere GFDL used the Australian bogus data for surface pressure; this is now known to be unreliable. The humidity fields in both analyses were strongly influenced by model physics.

A good indication of how well the assimilation system, forecast-analysis-initialization, performs is given by the magnitude of analysis increments. Fig.3 shows the mean height analysis increments at 500 mb during 1-20 May for the Final (a) and for the Main (b). Due to the improvements since the Main assimilation the mean increment is more than halved between South America and Africa. The overall pattern seems to be also much smoother and localized data problems associated with Indian radiosondes, Marion and Gough Island seem to cause smaller increments.

In the Main analysis the tropical convergence and divergence was damped by the adiabatic non-linear normal mode initialization, even if the 6h forecast and the subsequent analysis were able to create divergence/convergence. The amplitude of the divergent component of the analyzed flow is illustrated in Fig. 4a, which shows the mean analyzed velocity potential (00 and 12 GMT, 1-20 May 1979) for the Final ECMWF, Main GFDL and the Main ECMWF analyses. In Fig. 4a the convention selected is such that the divergent component of the flow is directed from low to high values of the velocity potential. For the Main ECMWF analyses the range of values is low, the maximum being 9×10^6 m^2 s^{-1} and minimum 22×10^6 m^2 s^{-1}. In the GFDL Main analyses the corresponding range is 23% higher and in the Final ECMWF 36% higher than in the Main ECMWF analyses. It can be clearly seen that circulations, of the Walker and Hadley type are more intense in the Final ECMWF compared with the Main ECMWF analyses, while the patterns have remained unchanged overall.

Fig. 4b shows mean zonal wind at 200 mb for the same period. The jet core is clearly stronger over North Africa and over Asia in the Final ECMWF than in the Main ECMWF which on the other hand is stronger than in Main GFDL. The same is true for the jet in the Southern Hemisphere. This can partly be explained by the fact that SATOB winds are not used north of 20N (except GOES-E/GOES-W) and are calibrated south of 20S (except GOES-E/GOES-W) and the slowing effect of SATOB data on strong winds has been avoided.

4.1 The fit of the analyses to data

These differences between the 3 sets of analyses arise because of the varying responses to data in the assimilations. Fig 5a-g provides a set of results which can help our understanding. In these figures there are two panels, the top panel comparing the Main and Final ECMWF analyses with observations and the bottom panel comparing the Main ECMWF and Main GFDL analyses. Slight differences in the results for the Main ECMWF analyses between the top and bottom panels arise because in the top panel we have used data accepted by the Final ECMWF as the verification data, while in the lower panel the data accepted by the Main ECMWF forms the verification data.

Within each panel there are three diagrams. On the right is a scatter diagram showing the fit of each analysis to the selected data, together with histograms formed by projecting the scatter diagram on one axis or the other. From each histogram an rms figure of the observation minus analysis differences is displayed. Thus in the upper panel in Fig 5a, the rms fit of the Final ECMWF to TEMP and PILOT wind reports at 200mb in the tropics is 5.53 m/s while the fit for the Main ECMWF analysis is 6.15m/s. In the lower panel we see that the Main ECMWF analysis fits the Main FGGE II-b data with an rms of 6.32 m/s, while the Main GFDL analysis fits the same data with an rms difference of 6.22 m/s. The differences in the fit of the Main ECMWF analysis to the "accepted" Main and Final FGGE II-b data (6.15 versus 6.32 m/s) gives some measure of the stability of the calculations. The verification period is May 1-20 1979.

The maps on the left, in Fig. 5a-g, show where one system fits the data closer than the other. Histograms were calculated for each 6-degree box, and the size of the plotted squares gives a measure of how often one system is closer to the observations than the other.

i) Tropical Results

Figs 5a-5d give results for the tropical belt 20S-20N, while Figs 5e-5g give global results. The quantity verified is either the 200 mb or 150 mb wind field. From Fig 5a we see that in almost all areas the Final ECMWF fits the TEMP and PILOT wind reports more accurately than the Main ECMWF. There is little difference in the behaviour of the Main GFDL and Main ECMWF in this regard.

Fig 5b shows the fit to aircraft data. In general the Final ECMWF fits the aircraft reports more accurately than the Main ECMWF (6.75 v. 7.44 m/s) over the tropical belt. The differences are most marked over the tropical Atlantic and Pacific where most of the data occurs. The Main ECMWF in turn fits the aircraft much more closely than the Main GFDL (7.55 v. 9.44 m/s), with most of the differences again occurring over the tropical Atlantic and Pacific.

Fig 5c shows the fit to the cloud track winds. In general the Final ECMWF analyses fit this data more closely in the tropics than the Main ECMWF (6.09 v. 6.54 m/s). The differences between the Main ECMWF and Final ECMWF are most marked in the Atlantic and Pacific, with little difference over the Indian Ocean. The Main ECMWF again fits the data more accurately than the Main GFDL analyses (6.63 v. 7.24 m/s). The differences in performance of the two systems are most clearly marked in the Indian Ocean, with the Main ECMWF consistently fitting the data more closely than Main GFDL.

Fig 5d (for 150mb rather than 200mb) shows the results for the constant level balloons. The Main ECMWF fits this data more tightly than the Final ECMWF almost everywhere (2.57 v. 3.16 m/s). Indeed we may suspect that the Main ECMWF analyses fitted this data too tightly. The differences in the treatment of this data between the Main and Final are trivial compared to the differences in the way it was handled by the Main GFDL system. The Main ECMWF is closer to this data in almost all cases, and the differences are substantial (2.76 v. 7.69 m/s).

The tropical results are summarised in table 2. For the period shown the Final ECMWF consistently fits the data more accurately than the Main ECMWF, except for the constant level balloons, where the differences are slight.

Comparison of the Main ECMWF and GFDL analyses shows that they both fit the TEMP AND PILOT wind reports to about the same degree. However the Main ECMWF is consistently closer to the aircraft, cloud-track wind and constant level balloon data in the tropics. These results appear to by typical.

ii) Global Results

Fig 5e shows the global results for the fit of the analyses to TEMP and PILOT wind reports. In general, the Final ECMWF uniformly fits this 200 mb wind data more closely than the Main ECMWF (5.3 v. 5.96 m/s). The isolated exceptions include a Brazilian station which was black-listed, and the isolated stations at Gough Island and Marion Island, whose directional biases were corrected before being used for the Final analysis. Since the verification is made using the original reports, the differences in treatment are clearly evident.

There is little difference in the overall fit of the Main ECMWF and GFDL analyses (6.11 v. 6.15 m/s) to the TEMP and PILOT wind reports. However many regional differences are evident. The Main ECMWF fits the East Pacific data, the Northern Chinese data and the North African data more tightly, while the Main GFDL fits the Australian, Middle Eastern, and Pakistan/ N W Indian data more tightly.

The differences in the treatment of tropical aircraft reports are also found in the global results, Fig 5f. The Final ECMWF consistently fits this data more closely than the Main ECMWF (7.7 m/s v. 8.35 m/s), with large differences occurring over all the oceans. Similarly, the Main ECMWF fitted the aircraft data on a global basis more accurately than the Main GFDL (8.42 v 10.52 m/s). The superiority of the fit of the Main ECMWF is clearly evident over all the oceans, and over land.

Finally we come to the global results for the SATOB (cloud drift wind) data, Fig 5g. The Main ECMWF analysis fits this data more tightly than the Final ECMWF (8.41 v. 9.82 m/s). The reasons are two-fold. The Final ECMWF did not use the data poleward of 20N, and the consequences are clearly evident in the maps. Poleward of 20S the data were calibrated for the Final ECMWF analyses. Since the verification is against the original reports, the Final ECMWF has

worse verification statistics in this region also. As noted already, in the tropical region where the data can be relied on, the Final ECMWF fits the data best. Comparison of the Main ECMWF and Main GFDL shows little global difference in the verifications (8.63 v. 8.64 m/s). There are, nevertheless, important regional differences. The superior fit of the Main ECMWF to the tropical data has already been noted. The neutral global result arises because the Main GFDL fits the cloud-wind data more closely near the main jets of both hemispheres. Since the data is known to have marked speed-dependent biases near the jets, an analysis which fits closely to the cloud-wind data in those regions is probably in error.

The global results are summarised in table 3. The Final ECMWF fits the high quality wind data in mid-latitudes (TEMPS, PILOTS, AIREPS) more closely than the Main ECMWF. The Main ECMWF in turn fits the high quality mid-latitude data better than the Main GFDL, particularly near the main jet streams. This is because the GFDL system, in effect, gives more weight to the low quality cloud-track winds near the jets, than the Main ECMWF; the cloud-wind data was discarded poleward of 20N, and calibrated poleward of 20S, in the Final ECMWF. This point is made quite succinctly in table 4 which shows the global verification figures for all three analyses. When the reported wind speed exceeds 25 m/s the Final ECMWF is closest to the high quality data and the Main GFDL is furthest from it. The positions are reversed for strong winds reported from the SATOB cloud-track winds. In the tropics, as we have seen already, the Final ECMWF out-performs the Main ECMWF, which in turn outperforms the Main GFDL, in the treatment of aircraft and cloud-track winds. The differences between the Final ECMWF and Main ECMWF in the treatment of constant level balloons in the tropics are small campared to the differences between the Main GFDL and Main ECMWF analyses.

We may therefore conclude that the Final ECMWF analyses are more faithful to high quality wind data than either the Main ECMWF or Main GFDL analyses, while the Main GFDL analyses are least faithful.

5. FORECAST EXPERIMENTS USING FGGE ANALYSIS

Of the few forecasts carried out with the N48 grid point model from Main ECMWF analyses one has been compared with a forecast for the Final analyses. Fig. 6 shows the anomaly correlation of geopotential height for the Northern Hemisphere produced by two forecasts run from 11 June 1979, 12Z. In this figure the full line is the correlation obtained with the T63 spectral model initialized with a Final analysis and the dashed line is the correlation obtained for the N48 model initialized with a Main analysis. This figure gives an illustration of the overall improvement of the system - the improvement of the data in the Final FGGE II-b data set, plus the improvement of the ECMWF analysis and forecast system between 1980 and 1985.

The results displayed in Fig. 7 gives an illustration of the impact of the additional data in the Final FGGE II-b dataset. This figure gives the scores for two forecasts run from 00Z 11 May 1979 using the T63 model, one run using a Main analysis and the other a Final analysis. Clearly the forecast from the more recent analysis is better. The improvements illustrated in Figs. 6 and 7 for Northern Hemisphere are substantial. In the Southern Hemisphere similar results have been obtained.

6. SATELLITE RETRIEVAL EXPERIMENT USING THE FINAL FGGE IIB DATA

The Final FGGE-IIb data set provides an excellent test bed for the evaluation of satellite temperature and humidity retrieval schemes. The data set contains both the NESDIS SATEM, temperature and humidity, data and clear-column (cloud-cleared) radiance data, both data having a horizontal resolution of 250 km. The SATEM data, consisting of temperature and humidity data for 14 thicknesses in the vertical (14 standard layers between 1000 and 10 mb), was derived from radiance data using a statistical retrieval technique. The present approach used at ECMWF, in common with many other operational centres, is to use the statistically derived SATEM data directly in the O/I analysis system. There are two known defects with this approach - SATEM data have large horizontally correlated errors near the tropopause and can, under some circumstances, have vertical structures which are inconsistent with those of the first guess used in an intermittent O/I procedure. These problems arise largely from the use of a climatological background field in the statistical technique used to produce SATEM data.

In order to improve the use of satellite data, two approaches are being evaluated in operational centres: (i) the direct use of the radiance data in an O/I analysis scheme; and (ii) the retrieval of temperature and humidity using a physical retrieval scheme in which the radiation transfer equation is "inverted" to obtain temperature and humidity profiles from prescribed (observed) radiances. The direct approach requires the determination of first guess radiances and statistics relating first guess radiance errors to first guess errors in model variables - wind, temperature and humidity; this would make the statistical retrieval an integral part of the analysis system, Durand (1985) and Kelly (1985). The physical retrieval approach requires a first guess for the vertical profiles of temperature and humidity in order to initiate an iterative evaluation of temperature and humidity from the radiation transfer equation.

In the past year a pilot study has been carried out in order to evaluate the benefits of using a physical retrieval package. The package used was the "EXPORT-2" scheme developed by the University of Wisconsin (see Smith, 1981), and the required first guess was the 6 hour forecast used in the Centre's data assimilation scheme. The period selected for this pilot study was 8-20 November 1979. This period, which has been used many times by other investigators for observing system tests (Baede (1985), Uppala (1984) and Kållberg (1984)), is a particularly good period for experimentation with satellite data; two polar orbiting satellites were operating reliably (TIROS-N and NOAA-6) and there was a strong circulation over the Atlantic.

The pilot study was comprised of two assimilation experiments - a control using NESDIS SATEM data and a physical retrieval experiment. Both assimilations were "cold-started" from climate fields at 00Z 8 November 1979 and the period 8-14 November was used to "warm-up" the assimilations and to "tune" the physical retrieval experiment. The performance of the two schemes were evaluated by comparing analyses, first guesses and retrieved profiles with observations and by comparing three 10-day forecasts (00Z 16 November, 12Z 18 November and 00Z 20 November, 1979) run from each assimilation.

6.1 Performance and evaluation of the assimilations

The similarity between sea-level pressure and geopotential height field analyses produced with the two experiments is striking. However, differences do exist in the temperature structures. These differences are illustrated in Fig. 8, which shows difference maps for geopotential thicknesses for 12Z 17

November 1979. As expected, the differences between the two assimilations are larger in the Southern than in the Northern Hemisphere and they are also larger for the 1000/700 mb thickness than for the 1000/500 mb thickness. This is a consistent feature of the differences between the two assimilations. In these experiments the retrieval techniques has had little impact on geopotential height or on large thicknesses, but had a large impact on thin layers and on details in the vertical structure of the temperature field.

The fit of the 6 hour forecasts to SATEMs is more accurate in the physical retrieval assimilation than in the control - this can of course be expected since the 6 hour forecasts provided the first guess below 100 mb for the retrieval algorithm. The fit of the 6 hour forecasts to radiosonde data is similar for both experiments, with the physical retrieval system performing better in the troposphere and worse in the stratosphere, this is illustrated in Fig. 9.

Although the forecasts from the two assimilations are similar to day 3, the physical retrieval forecasts are on average worse than those made from the control assimilations. The anomaly correlation of geopotential height, shown in Fig. 10, for the 12Z 18 November case is an illustration of the differing level of performance. This negative impact of the physical retrieval scheme, although small, has been traced back to two different problems - one is associated with the use of satellite data in the stratosphere and the other is the first guess used to initialize the physical retrieval scheme.

6.2 Problems and proposals for further experimentation

To be successful a physical retrieval scheme requires a first guess which is of reasonable accuracy. In particular, large biases in the first guess leads to biased retrievals and subsequently biased analyses. During the tuning period such a problem emerged in the stratosphere, because of the poor quality of the first guess (6 hour forecast) temperature field above 100 mb. In the physical retrieval experiment, this problem was partially alleviated by using the NESDIS SATEMs as the first guess above 100 mb and the 6 hour forecast below 100 mb. However, the poor quality of the stratospheric first guess still caused the stringent tests applied in the physical retrieval experiment to discard large amounts of satellite radiance data in the stratosphere. Consequently the physical retrieval experiment had less data in the stratosphere than the control and this led, in some areas, to surprisingly

large differences between the two sets of analyses (e.g. the 100/50 mb layer is 8°K colder in the physical retrieval experiment than in the control over Antarctica on 18 November 1979 00Z). This explains why the fit of the first-guess to the radiosonde data is less good in the stratosphere for the physical retrieval experiment (Fig. 9).
In contrast, for the troposphere the use of a physical retrieval scheme leads to an improvement in the fit to radiosonde data (Fig. 9). Locally, the improvement can be large. Fig. 11 shows a comparison between the NESDIS SATEMS, a satellite sounding produced with the physical retrieval scheme and a collocated radiosonde observation (Ship (P) PAPA); the physical retrieval sounding, presumably "helped" by the first guess, is much closer to that of Ship P. On average, the differences between NESDIS and the physically retrieved soundings are of course smaller than those depicted in Fig. 11. However, Fig. 11 provides an illustration of the differences that occur in data sparse areas. Compared with the statistical retrievals (SATEMS), the quality of the physically retrieved data is considerably better provided the first guess is of a reasonable quality.

Some aspects of the poor performance in the forecasts made from the physical retrieval analyses have been traced back to specific areas (North polar cap, mid-Pacific ocean) where the first guess appears to be incorrect by several degrees K. In these situations the physically and the statistically retrieved soundings differ significantly and the soundings derived using the physical retrieval are almost identical to the first guess (see Fig. 12). This is an example of an "incest" problem in which a poor first guess is as a consequence uncorrected and retained throughout the assimilation process.

The influence of the first guess humidity field also had a significant impact on the humidities retrieved with the physical retrieval package. In the troposphere the first guess humidities were found to be too moist with a large gradient of humidity at about 700 mb over a 100 mb layer. Since the EXPORT-2 package can only correct moistures over deep layers, this gradient remained as a persistent feature of the physical retrieval assimilation.

It is clear from this pilot experiment that the quality of the first guess is crucial for the satisfactory performance of a physical retrieval scheme. Where the first guess is reasonable, the physically retrieved soundings are more accurate than the NESDIS SATEMS, but where there are biases or large

inaccuracies in the first guess the physically retrieved soundings can be degraded significantly.

In the near future these experiments will be repeated using the new 19-level data assimilation system - this will reduce the stratosphere problem significantly. For the longer term it is planned to tackle the "incest" problem for physical retrieval schemes and to evaluate schemes which use satellite radiances directly in the analysis procedure.

7. SUMMARY

At the time of writing only a preliminary analysis of the Final FGGE III-b analyses has been possible. Compared with the Main FGGE III-b analyses, the Final FGGE III-b analyses are considerably improved. The improvements have resulted from:

- the additional observations
- better use of observations
- and improvements in the assimilation system.

The positive impact of the extra data and of the improvements in the moisture analysis, is most obvious in the tropics. In the Northern Hemisphere where the data coverage was already good in the Main FGGE II-b data set, the way the data set is assimilated appears to be an important factor for the quality of forecasts.

The FGGE II-b and III-b data will continue to provide data sets for experimentation at ECMWF for many years to come, particularly for observing system experiments and satellite data studies.

REFERENCES

Baede, A.P.M., P. Kållberg and S. Uppala, 1985: Impact of aircraft wind data on ECMWF analyses and forecasts during the FGGE period, 8-19 November 1979. ECMWF Tech.Rep.No.47.

Durand, Y., 1985: The use of satellite data in the French high resolution analyses. ECMWF Workshop on High Resolution Analysis (June 1985) 89-128.

Illari, L., 1985: The quality of ECMWF humidity analysis. ECMWF workshop on High Resolution Analysis (June 1985).

Kållberg, P., 1984: Performance of some different FGGE observation subsets for a period in November 1979. ECMWF Seminar/Workshop 1984: Data assimilation systems and Observing System Experiments with particular emphasis on FGGE, 203-228.

Kållberg, P., 1985: On the use of cloud track winds data from FGGE in the upper troposphere. ECMWF Research Department Tech.Memo No.110.

Kelly, G., 1985: The use of satellite radiance measurements in the ECMWF analysis system. ECMWF Workshop on High Resolution Analysis (June 1985), 27-40.

Pasch, R. and L. Illari, 1985: FGGE moisture analysis and assimilation in the ECMWF system. ECMWF Tech.Memo.No.110.

Shaw, D., P. Lönnberg and A. Hollingsworth, 1984: The ECMWF Research Department Tech.Memo. No.92 (also submitted to QJRMS (1986)).

Smith, W., H.M. Woolf, C.M. Hayden, A.J. Schreiner and J.M. Le Marshall, 1983: The physical retrieval TOUS export package. First TOVS study conference, Igls, Austria, 1983.

Tiedtke, M. and J. Slingo, 1985: Development of the operational parameterization scheme. ECMWF Tech.Memo.No.108, 38pp.

Uppala, S., A. Hollingsworth, S. Tibaldi and P. Kållberg, 1984: Results from two recent observing system experiments at ECMWF. ECMWF Seminar/Workshop 1984: Data assimilation systems and Observing System Experiments with particular emphasis on FGGE, 165-202.

Wergen, W., 1982: Initialisation. ECMWF Seminar/Workshop 1982: Interpretation of Numerical Weather Prediction Products, 31-57.

		FINAL ECMWF	MAIN ECMWF	MAIN GFDL
200 mb	TEMP, PILOT	5.5	6.2	6.2
	AIRCRAFT	6.8	7.6	9.4
	SATOB	6.1	6.6	7.2
	CONSTANT-level Balloons	3.2	2.7	7.7

Table 2 Tropics (20°S - 20°N) rms of vector wind difference (OBS-ANAL) (m/s)

		FINAL ECMWF	MAIN ECMWF	MAIN GFDL
200 mb	TEMP, PILOT	5.3	6.1	6.2
	AIRCRAFT	7.7	8.4	10.5
	SATOB	9.8	8.6	8.6

Table 3 Global rms of vector wind difference (OBS-ANAL) (m/s)

		FINAL ECMWF	MAIN ECMWF	MAIN GFDL
200 mb	TEMP, PILOT	6.6	7.7	7.9
	AIRCRAFT	9.2	10.1	12.6
	SATOB	10.6	9	8.7

Table 4 Jets Observed Wind > 25 m/s rms of vector wind difference (OBS-ANAL) (m/s)

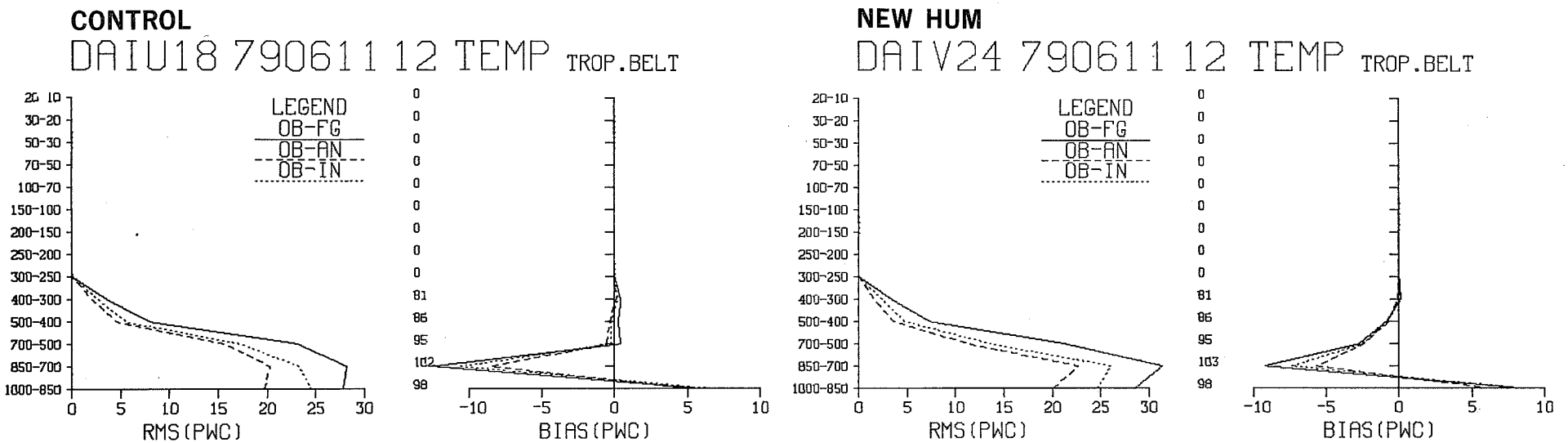

Fig. 1 rms/bias of the deviations between the radiosonde Precipitable Water Content observations and the first guess (----), the analysis (----) and the initialisation (.....).

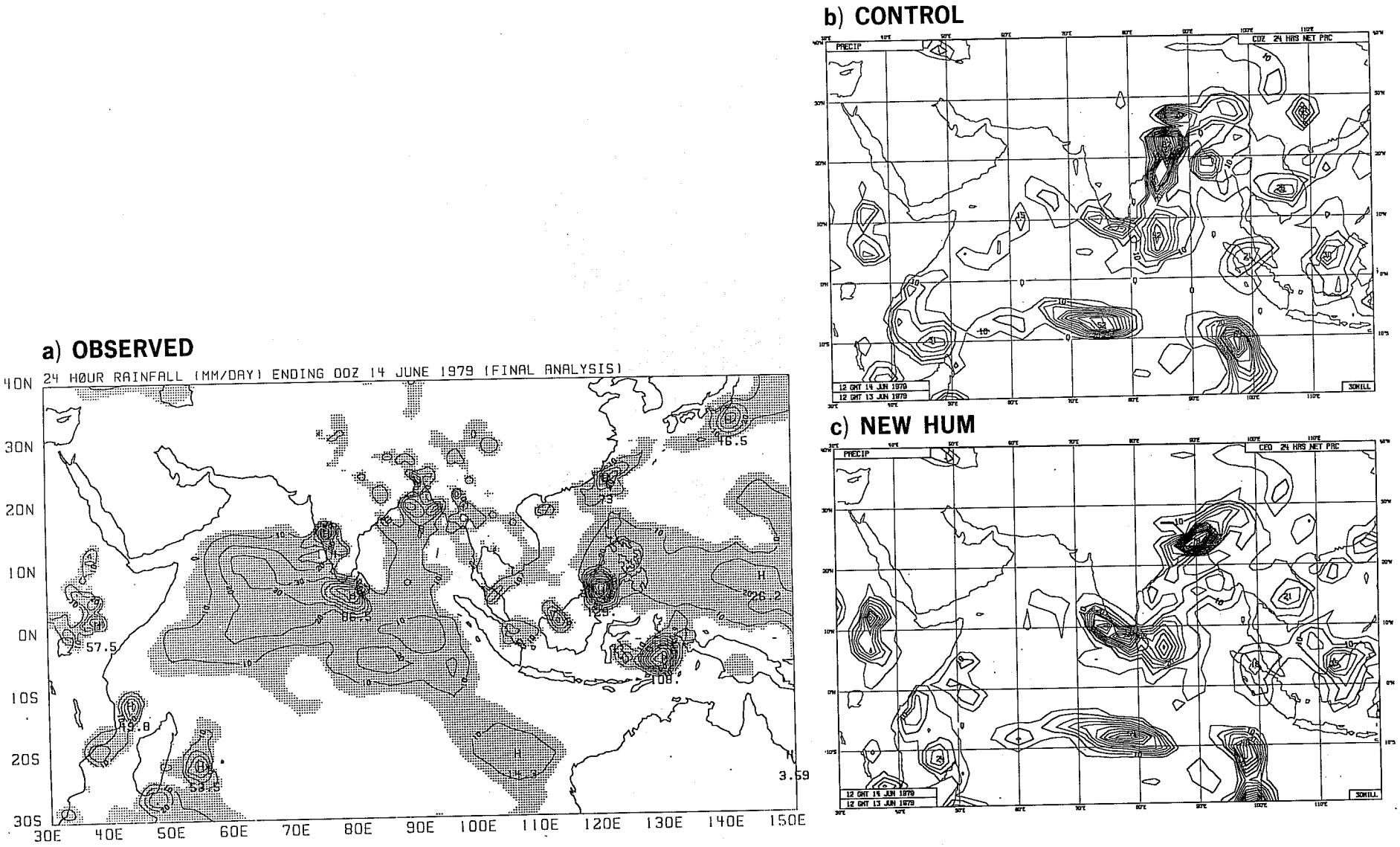

Fig. 2 **24h accumulated rainfall after 2½ days in the forecast from 11 June 1979 12Z.**

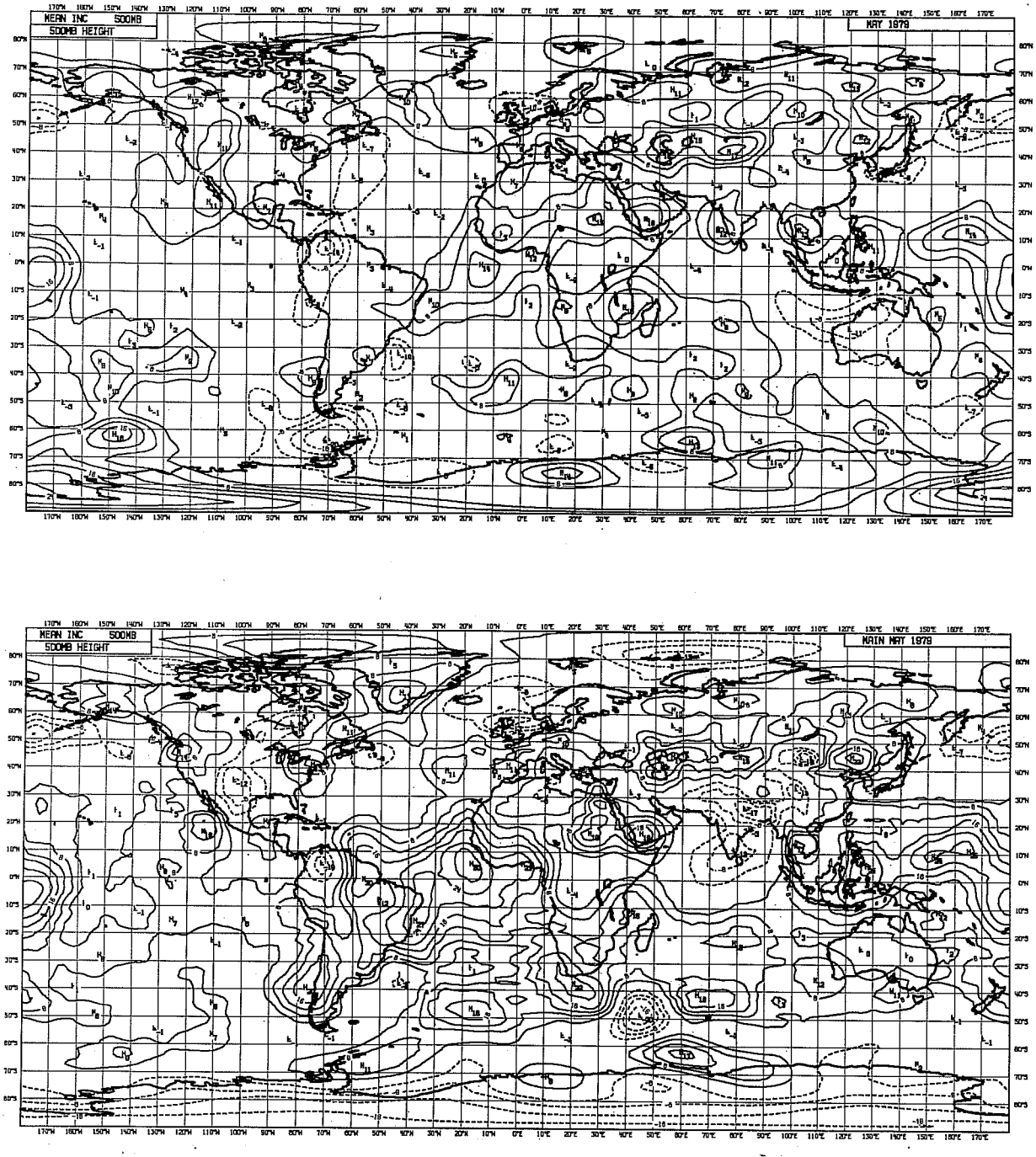

Fig. 3 500 hPa geopotential height increment maps.
Mean analysis increments accumulated in the period 1-20 May 1979 for the Main (bottom panel) and Final (top panel) III-b analyses.

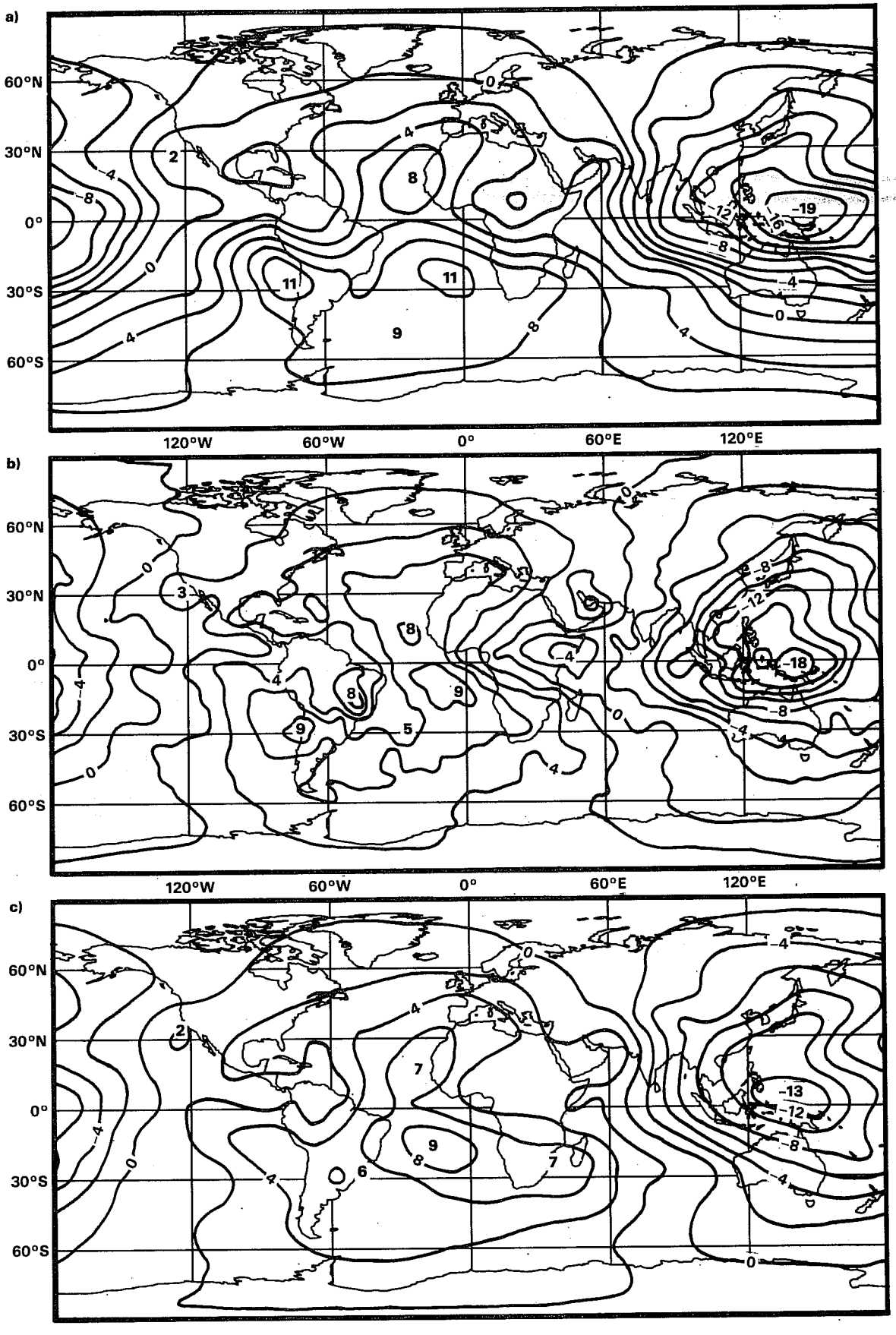

Fig. 4a Mean 200 hPa velocity potential maps accumulated in the period 1-20 May 1979 for the final ECMWF FGGE analysis (top), the main GFDL Analysis (middle) and the ECMWF main analysis (bottom).

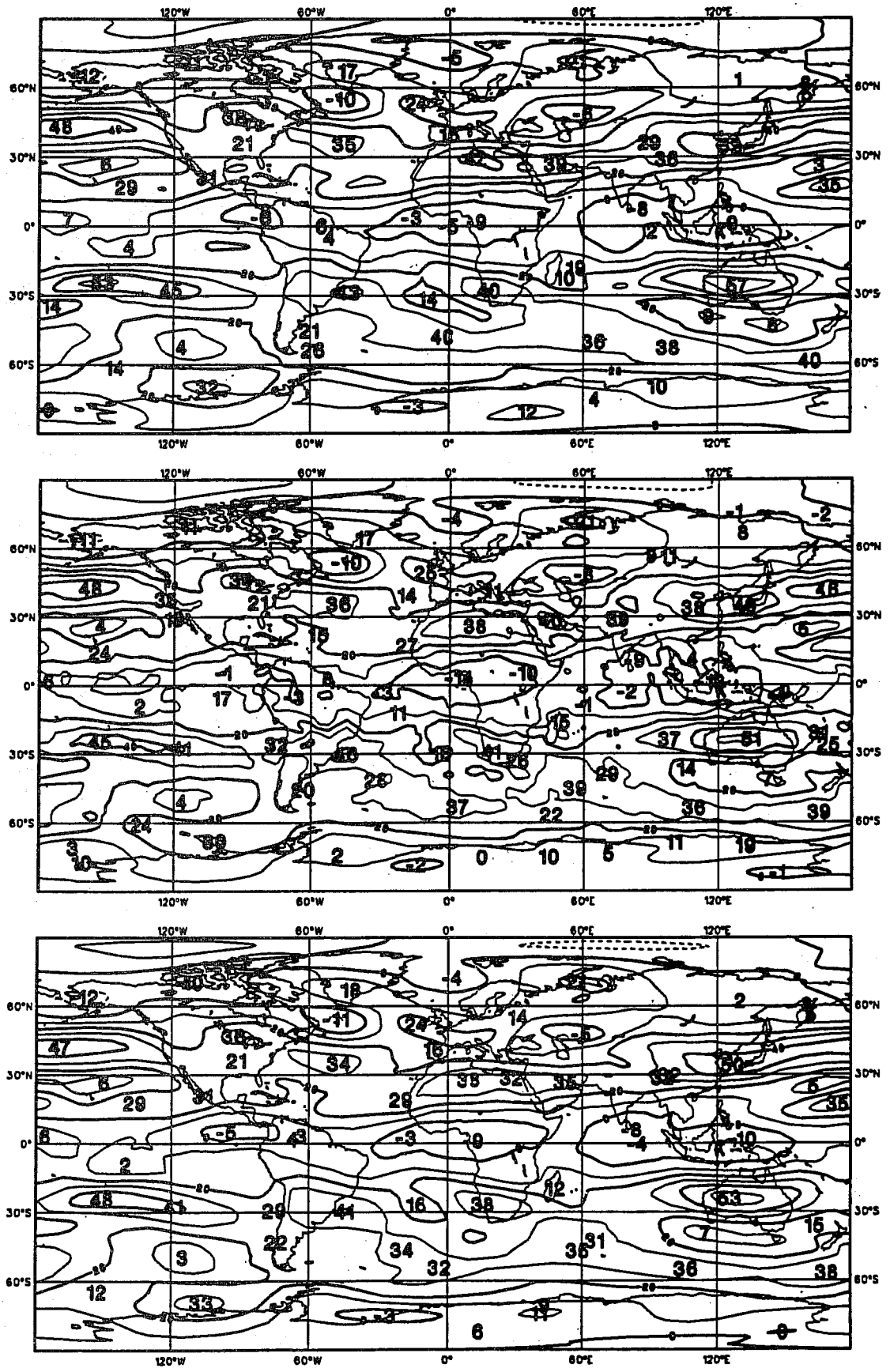

Fig. 4b Mean 200hPa wind speed accumulated in the period 1-20 May 1979 for the final ECMWF FGGE analysis (top), the main GFDL analysis (middle) and the ECMWF main analysis (bottom).

Fig 5. Each of the figures, Fig. 5a-5g shows comparative verification results for the Final ECMWF and Main ECMWF analyses (top panels) and Main ECMWF and Main GFDL (bottom Panels).

Each panel contains three diagrams. On the right is a scatter diagram showing the histograms of (Observation - Analysis) differences for the magnitude of the vector wind difference. The vertical axis shows the results for the Main ECMWF in all cases. A horizontal (vertical) line is drawn to indicate the rms value of the differences plotted on the vertical (horizontal) axes, and the line is labelled accordingly. The histograms provide comparisons of the two sets of (Observation - Analysis) differences.

The maps on the right of each panel show where one analysis performs better than the other. For each 6 degree box a count is made of the number of times one analysis fits the data closely than the other. The size of the black area in the box is proportional to the number of occassions in the 20 day period (1-20 May, 4 analyses per day) when the specified analysis was closer to the observations. The verification parameter is 200mb vector wind, apart from Fig 5d where it is 150mb wind. The verification data and areas are as follows:

a) 20N-20S, temps and pilots

b) 20N-20S, aircraft

c) 20N-20S, cloud track winds

d) 20N-20S, constant level balloons, 150mb

e) Global, temps and pilots

f) Global, aircraft

g) Global, cloud track winds

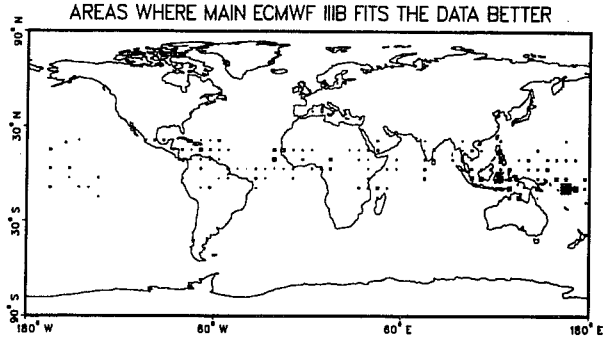

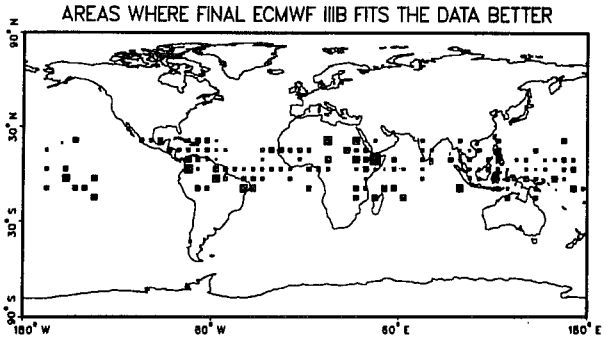

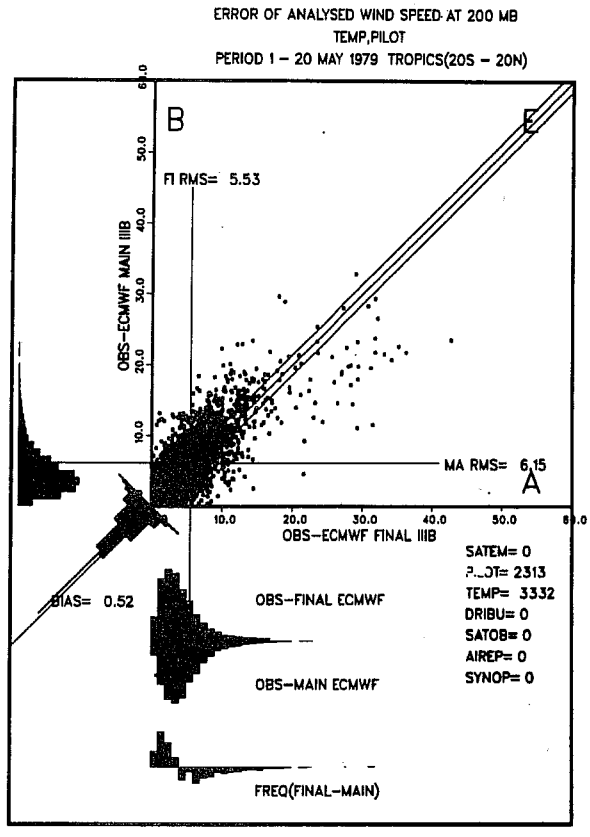

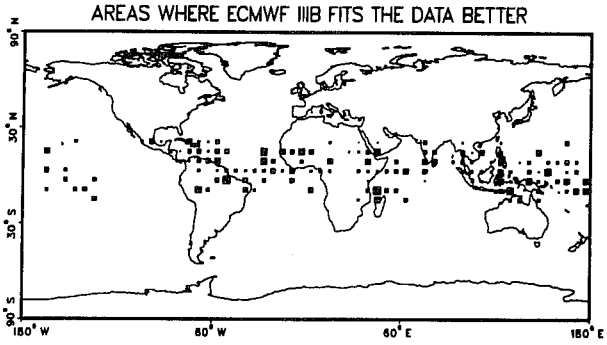

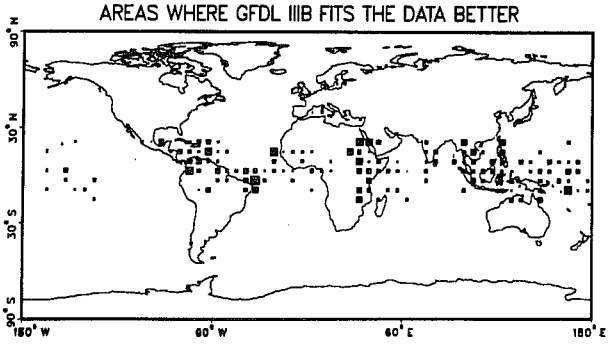

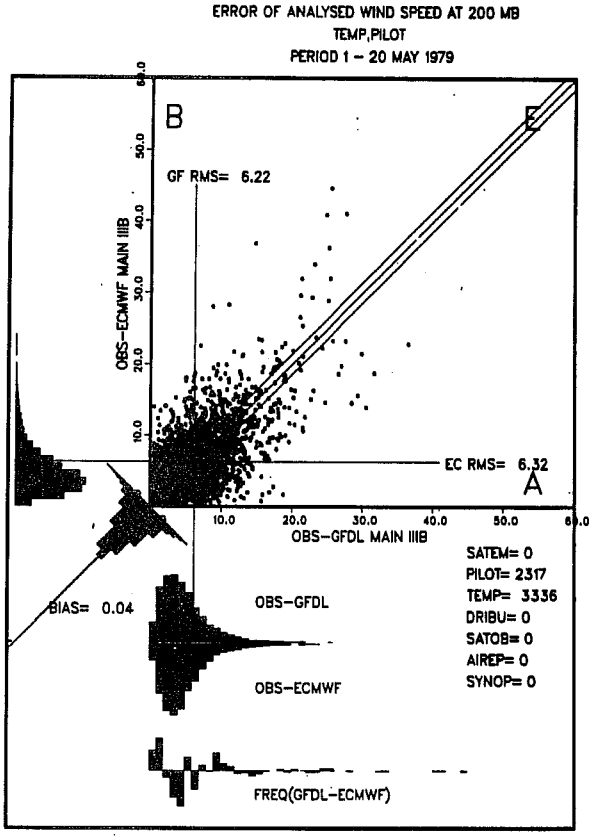

a) 20N-20S, temps and pilots

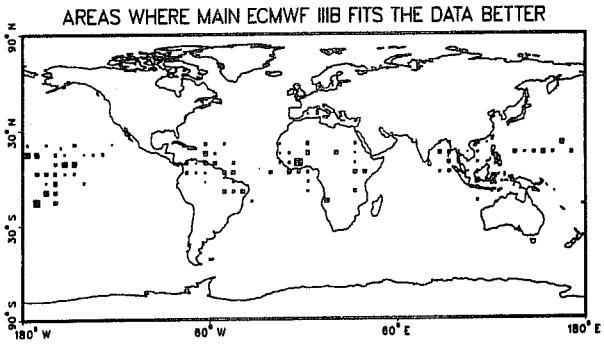

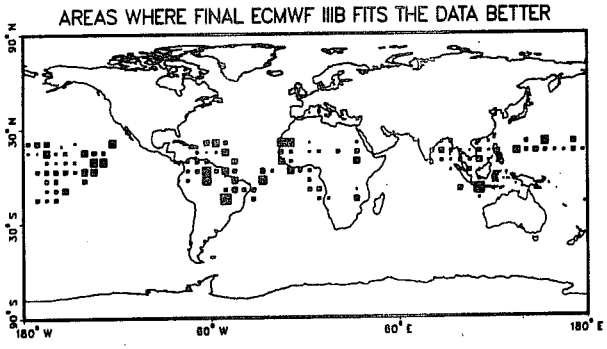

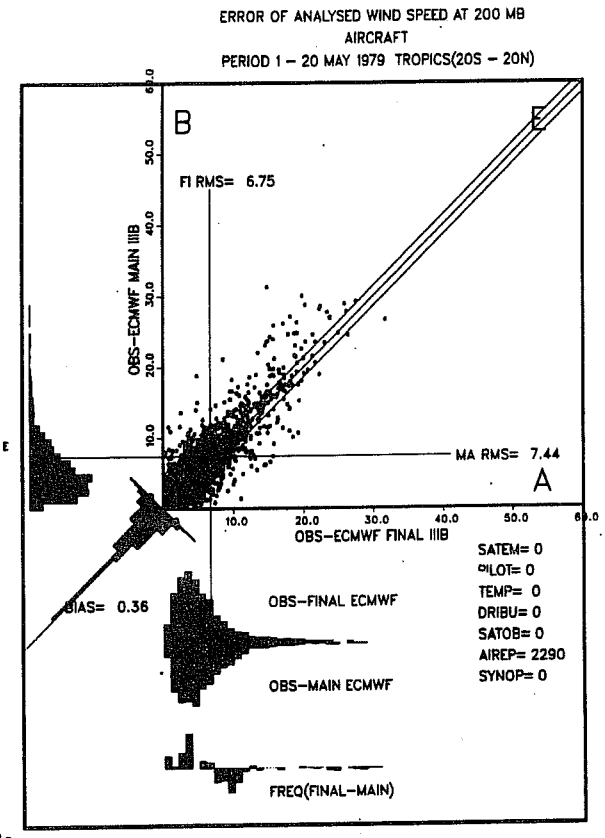

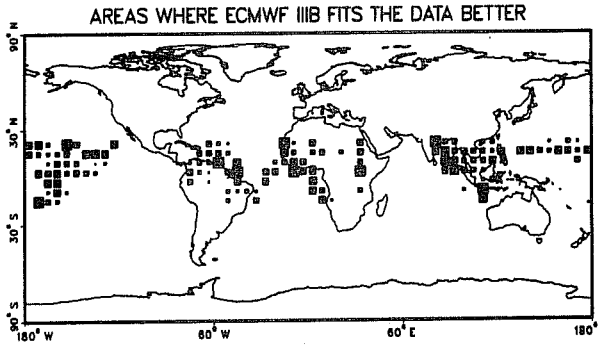

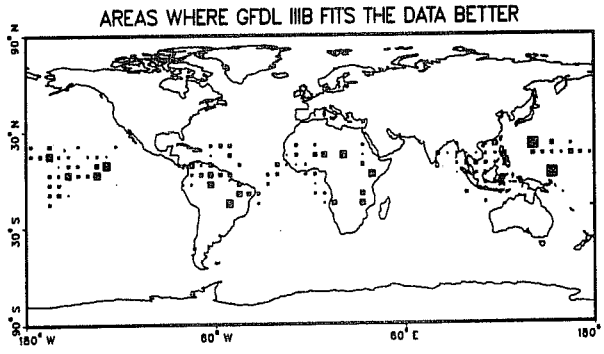

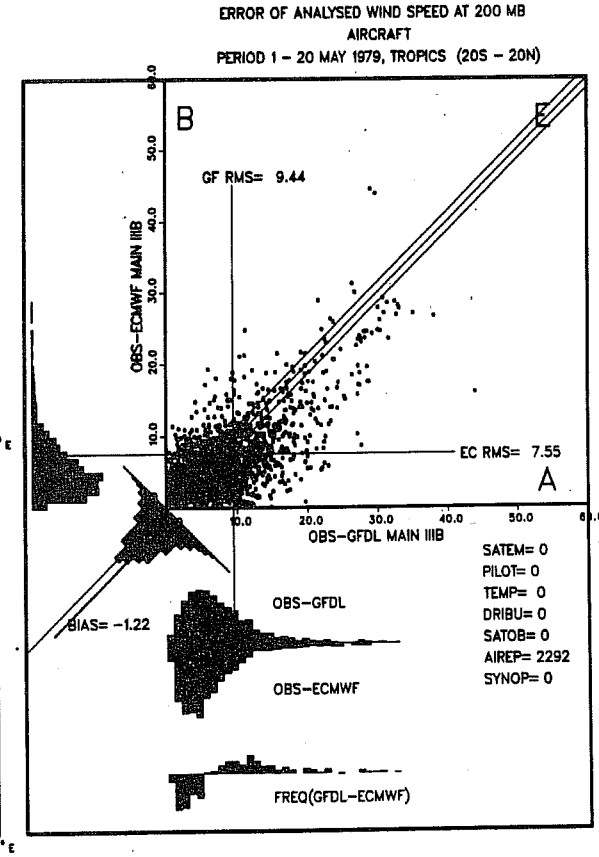

b) 20N-20S. aircraft

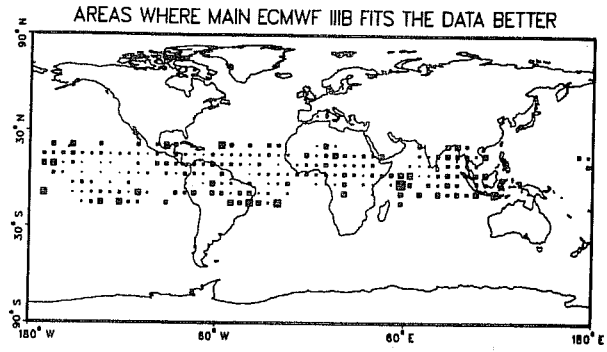

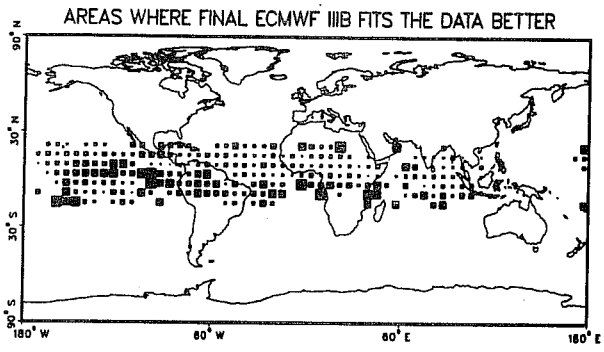

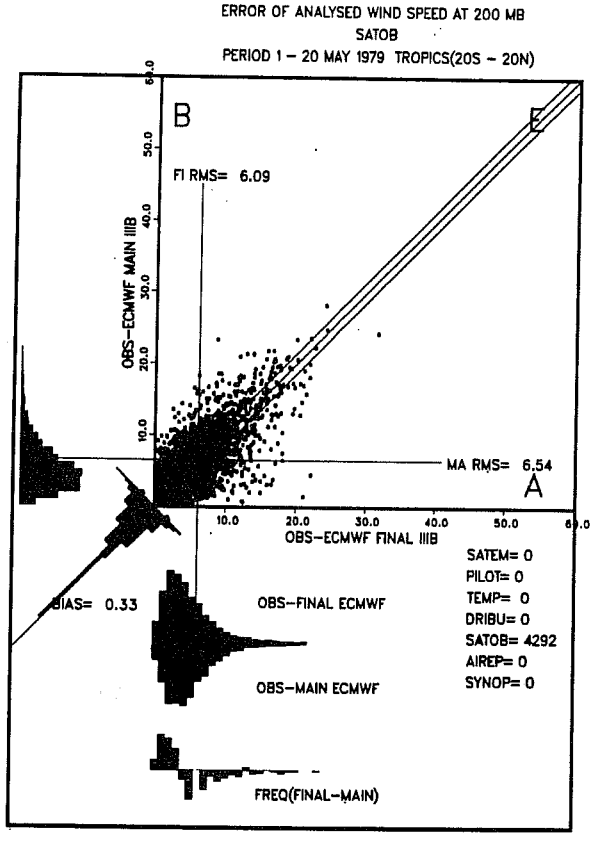

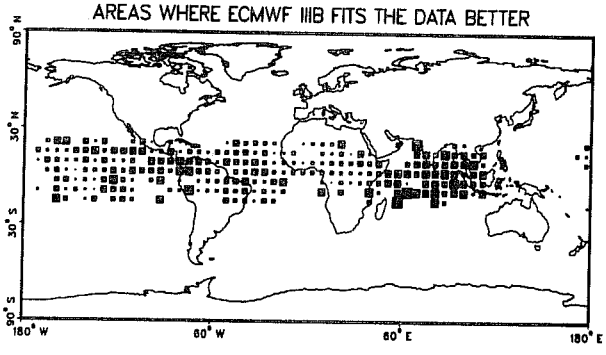

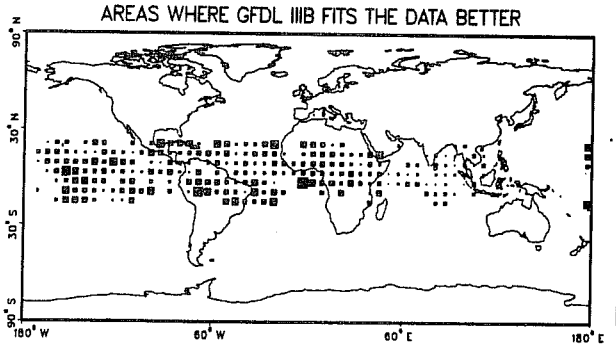

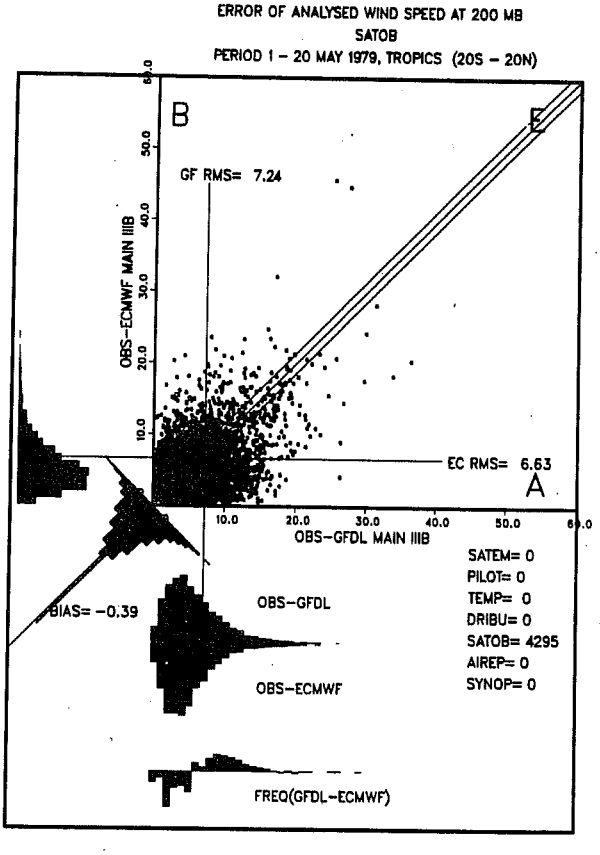

c) 20N-20S, cloud track winds

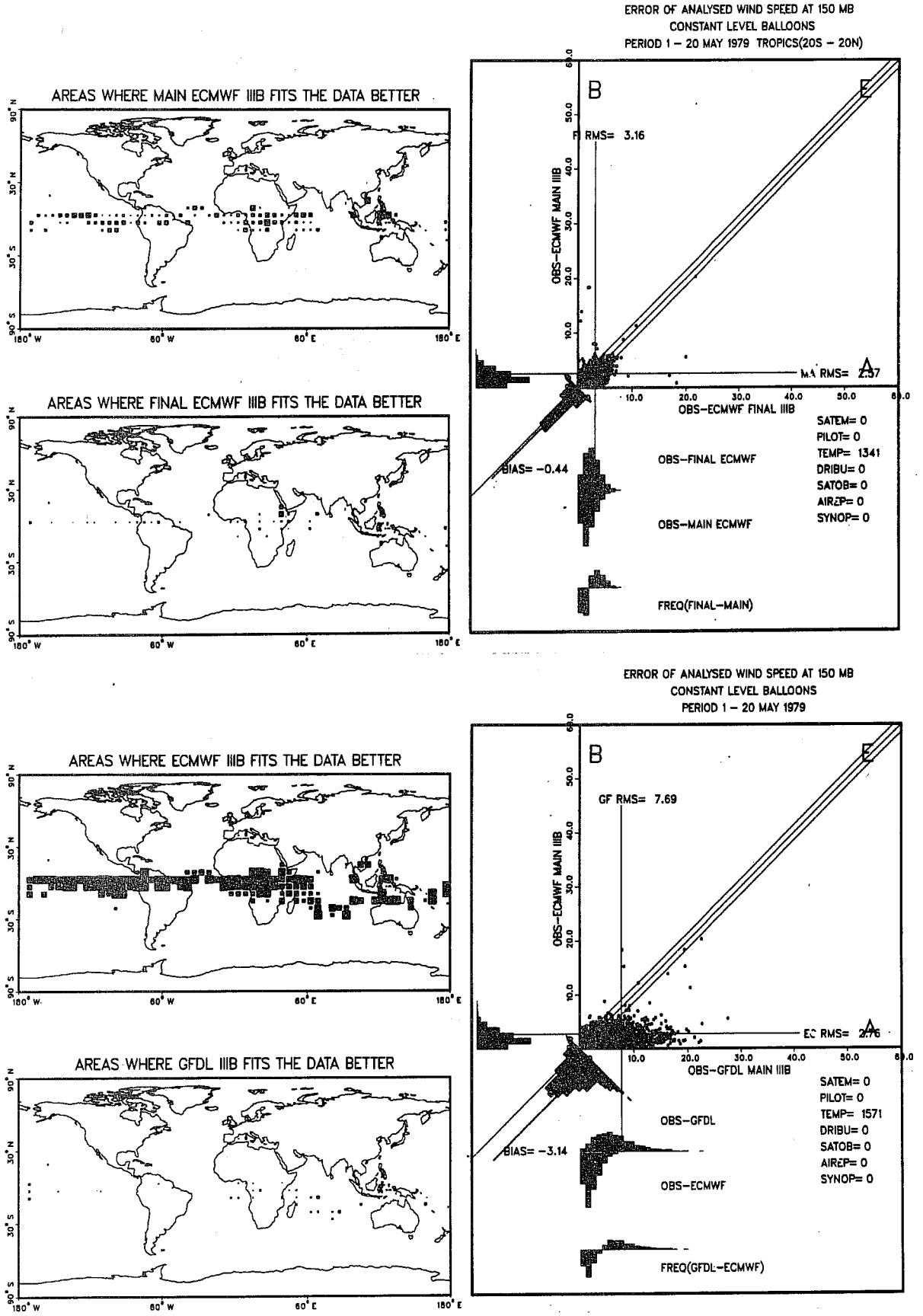

d) 20N-20S, constant level balloons, 150mb

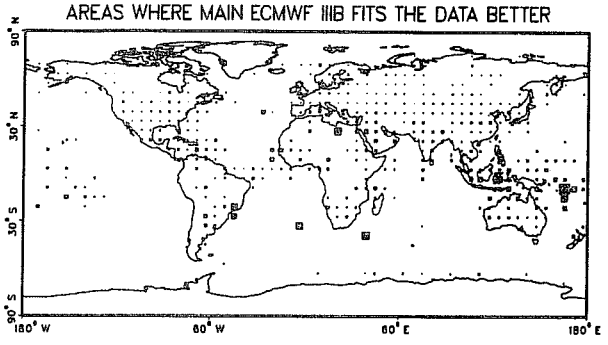

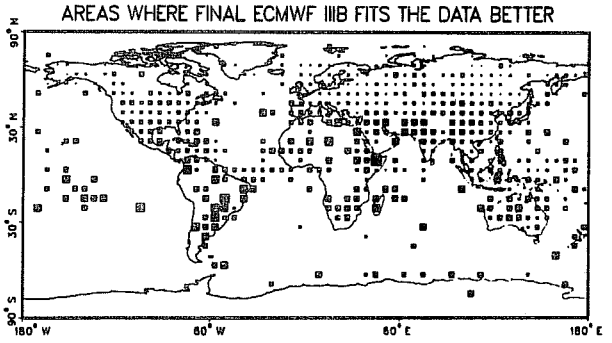

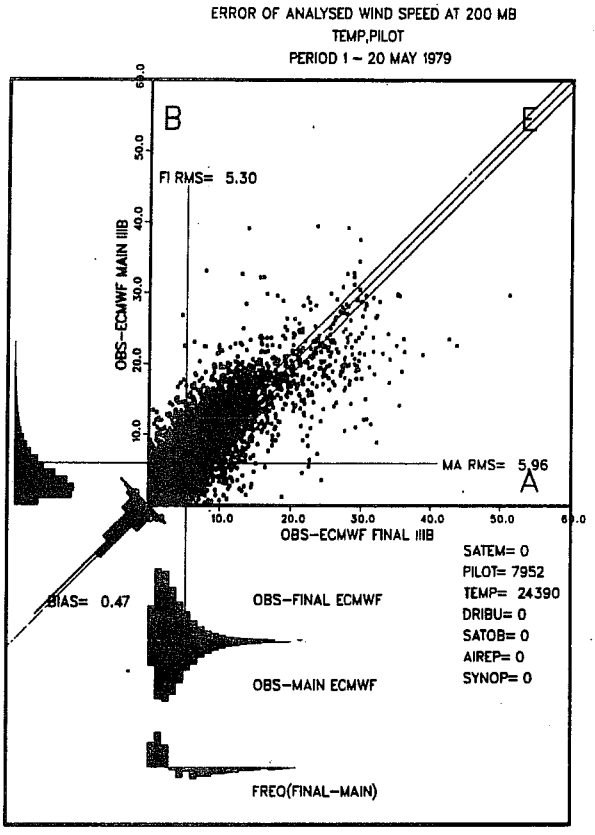

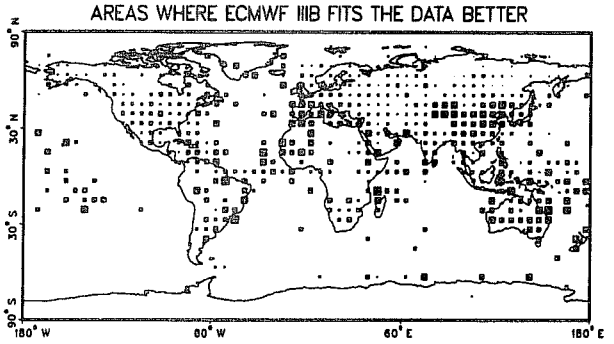

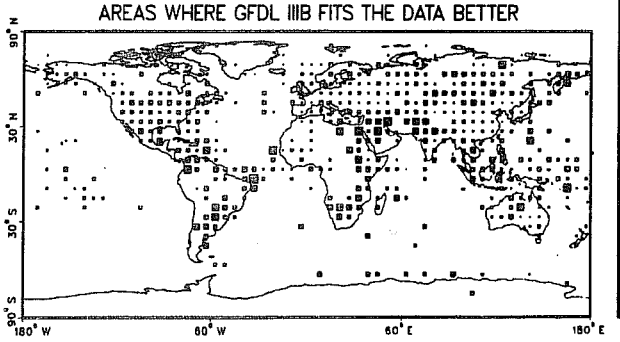

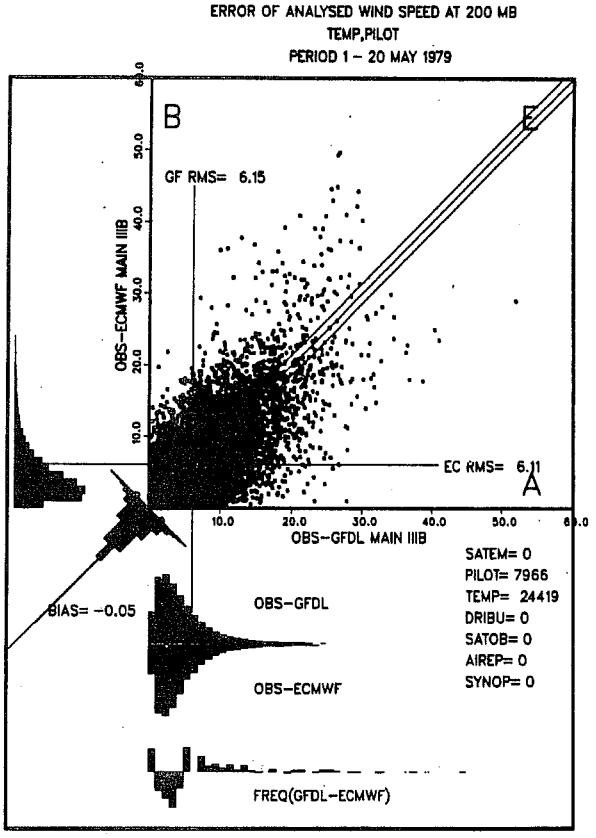

e) Global, temps and pilots

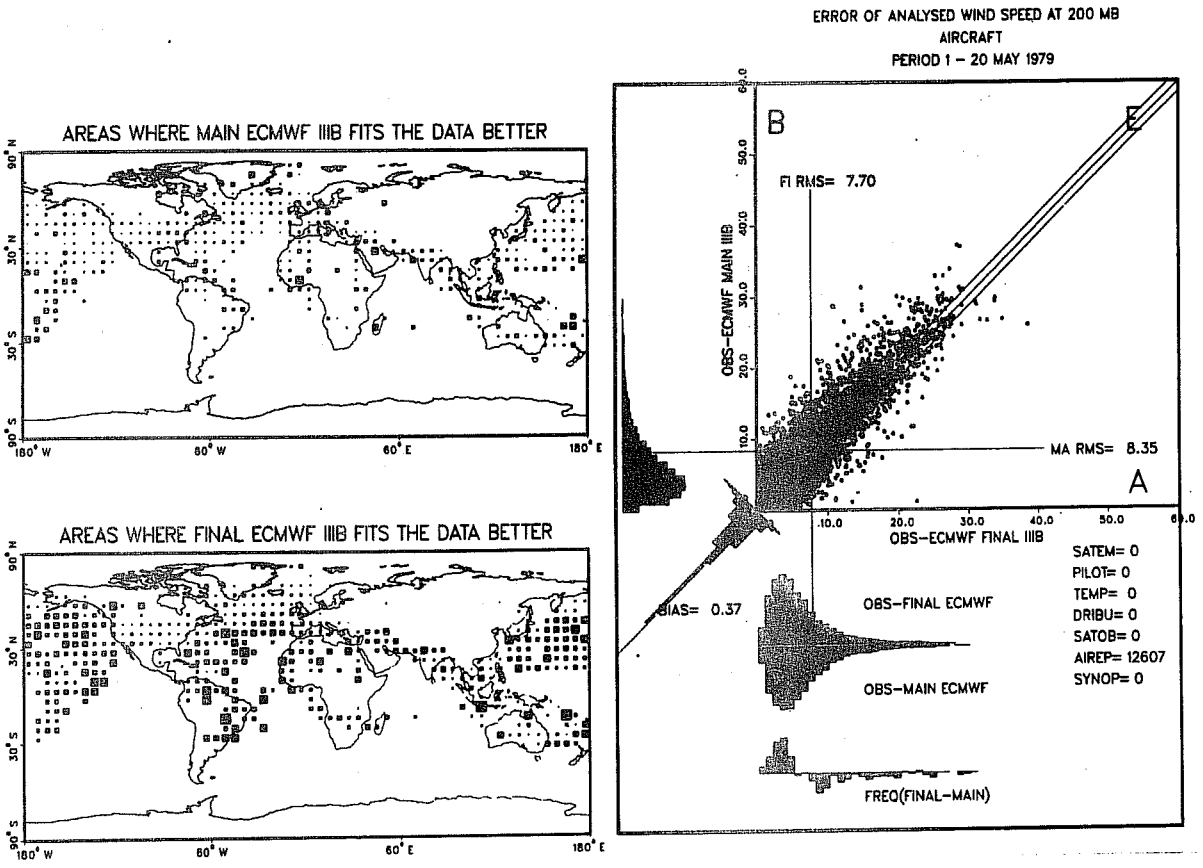

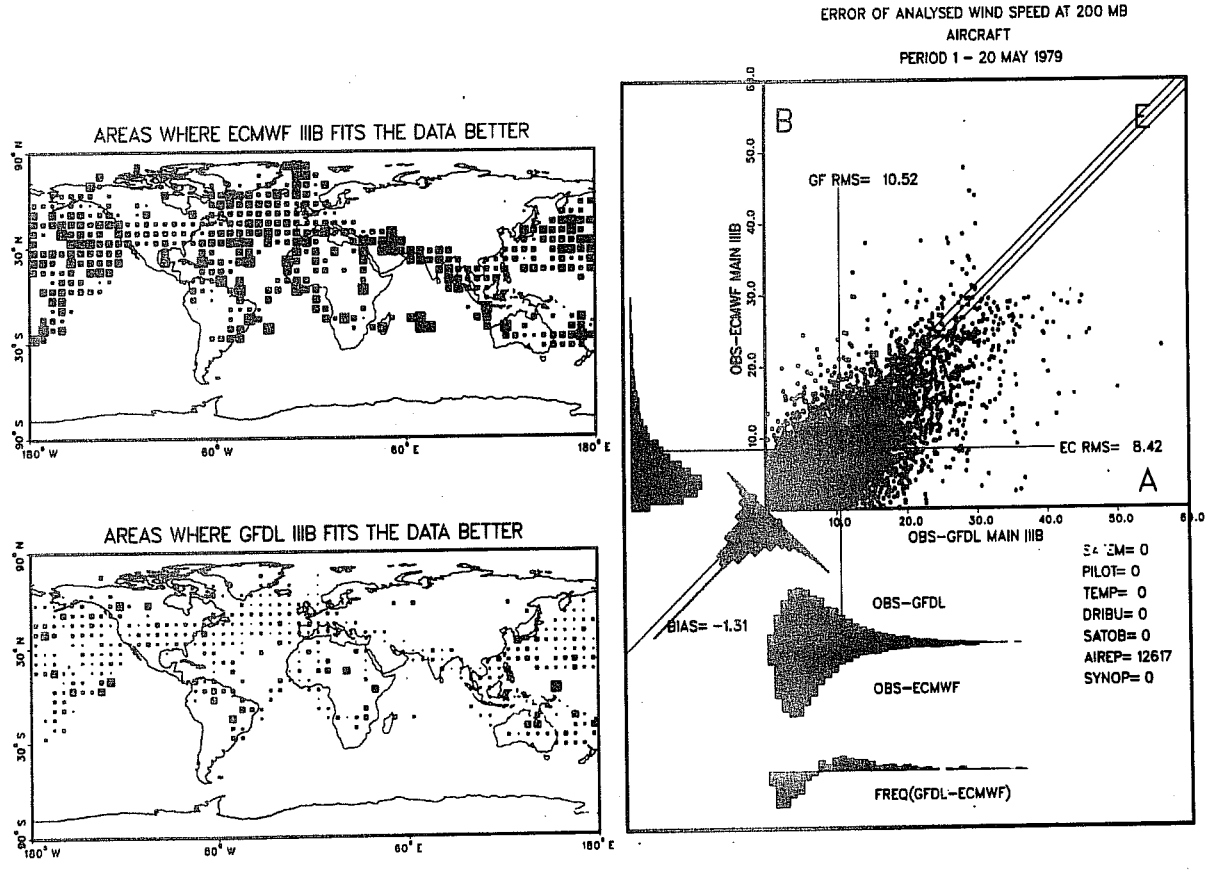

f) Global, aircraft

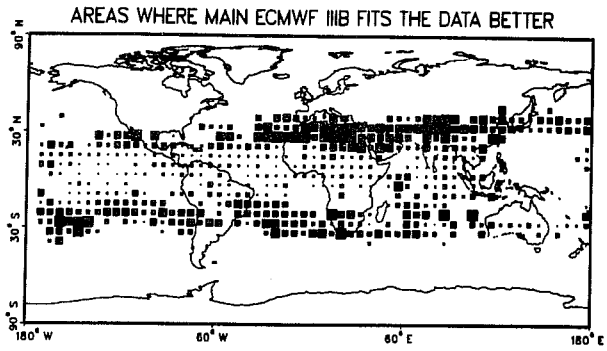

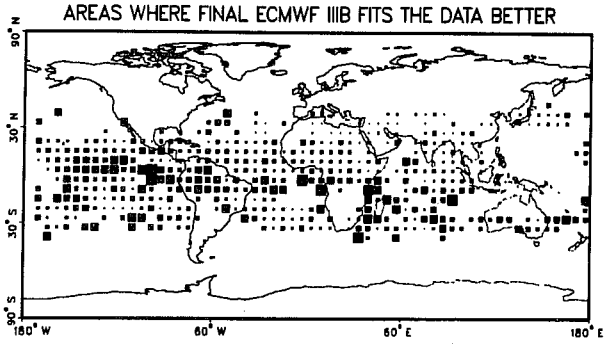

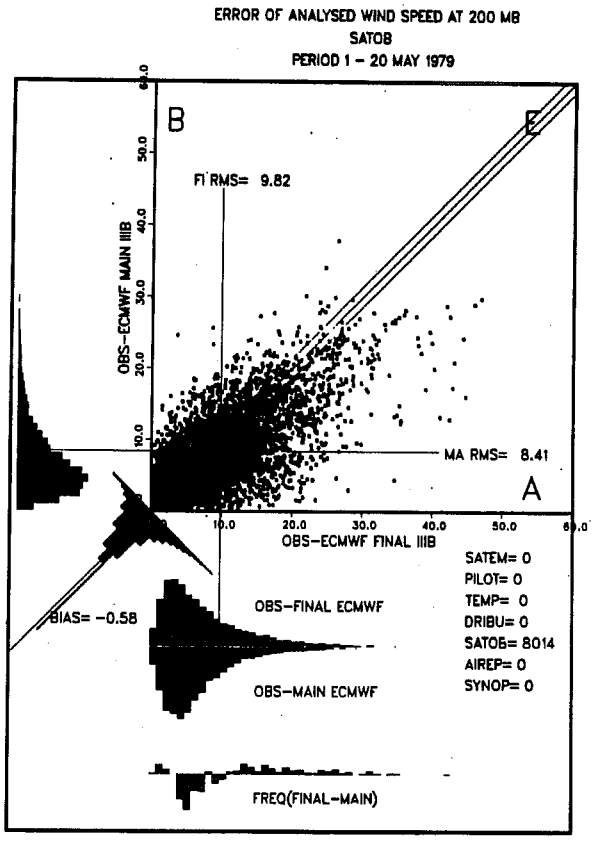

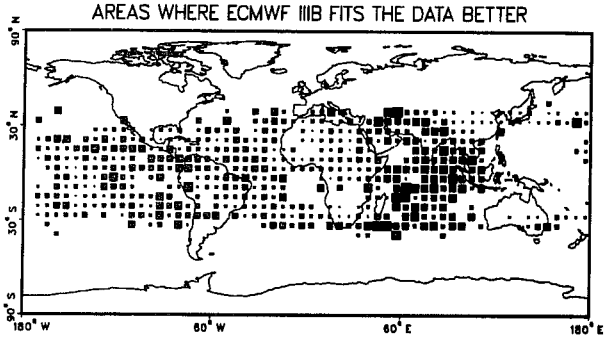

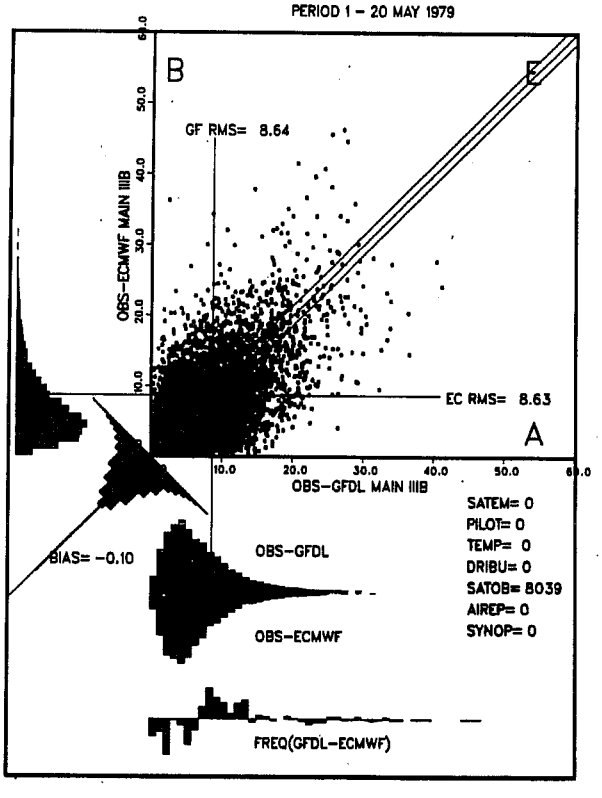

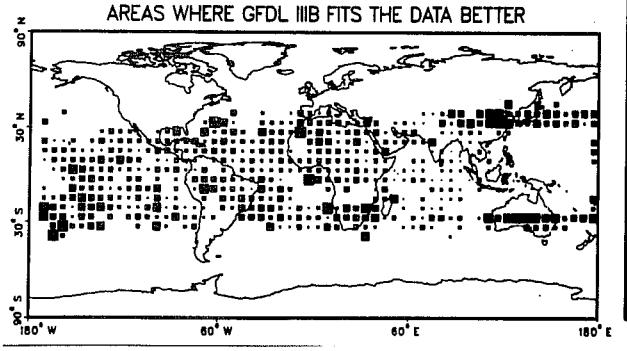

g) Global, cloud track winds

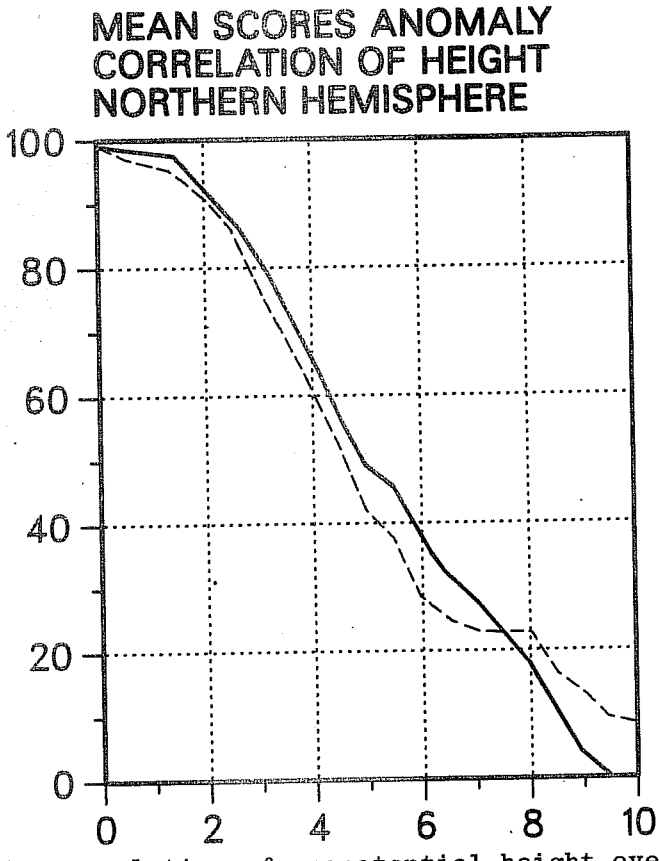

Fig. 6 Anomaly correlation of geopotential height over Northern Hemisphere for two forecasts run on 11 June 1979, 12Z
Full line: T63 on Final analysis Dashed line: N48 on Main analysis

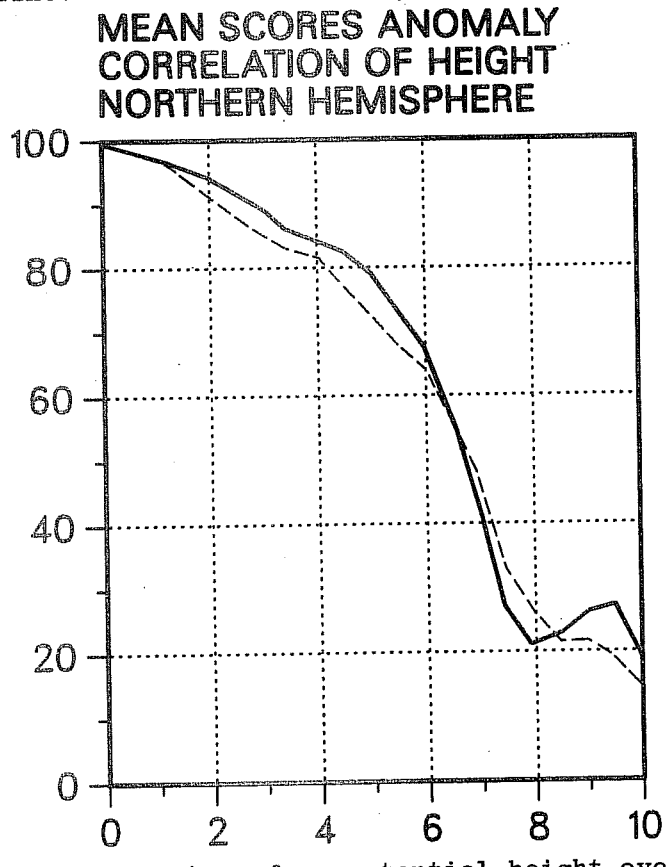

Fig. 7 Anomaly correlation of geopotential height over Northern Hemisphere for two forecasts run on 11 May 1979, 00Z
Full line: T63 on Final analysis Dashed line: T63 on Main analysis

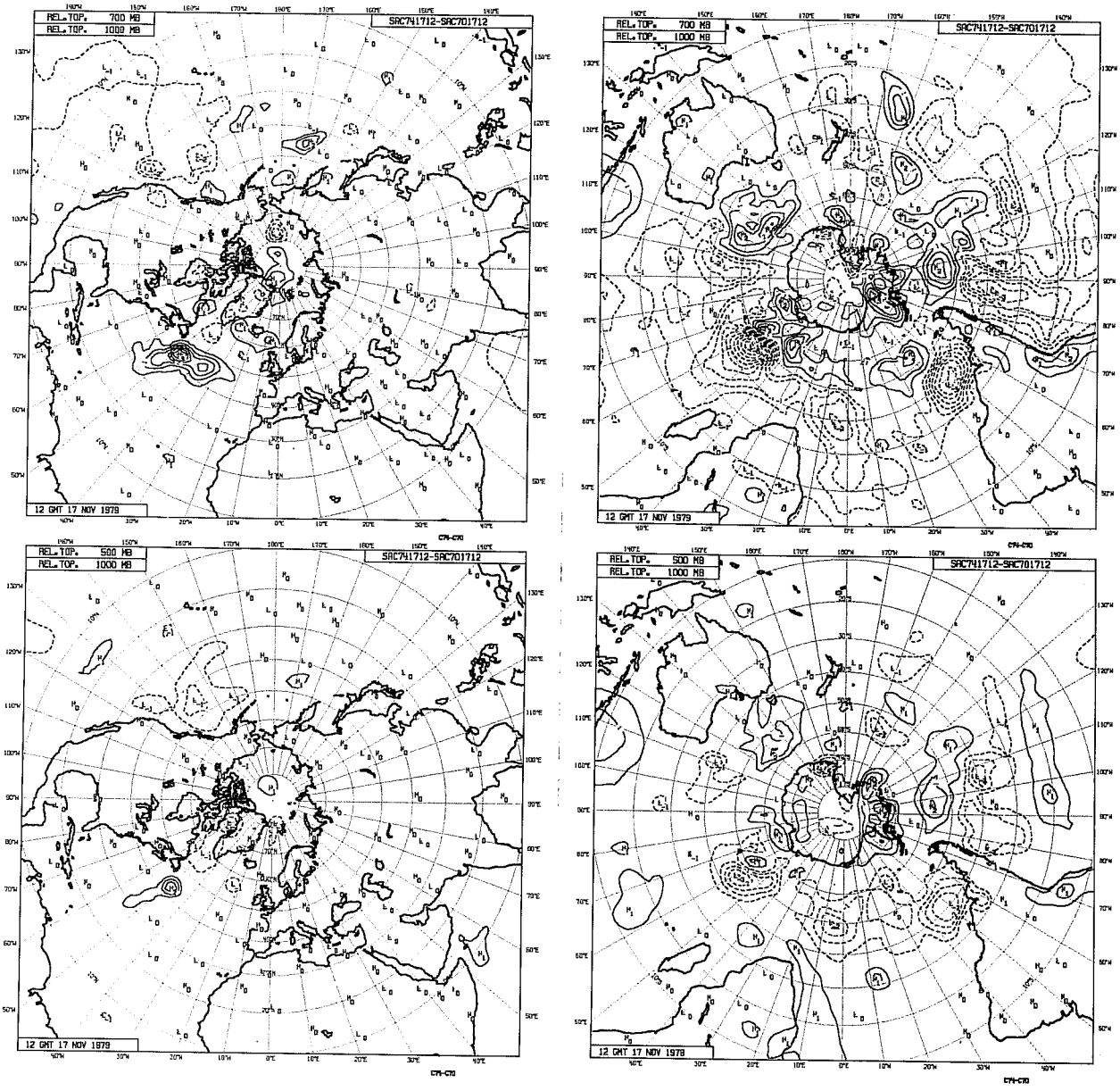

Fig. 8 Difference maps between the "physical retrieval" analysis and the control analysis on 17 November 1979 12Z. Top: 1000/700 thickness - Bottom: 1000/500 thickness. Left: Northern Hemisphere - Right: Southern Hemisphere. Unit: decameter.

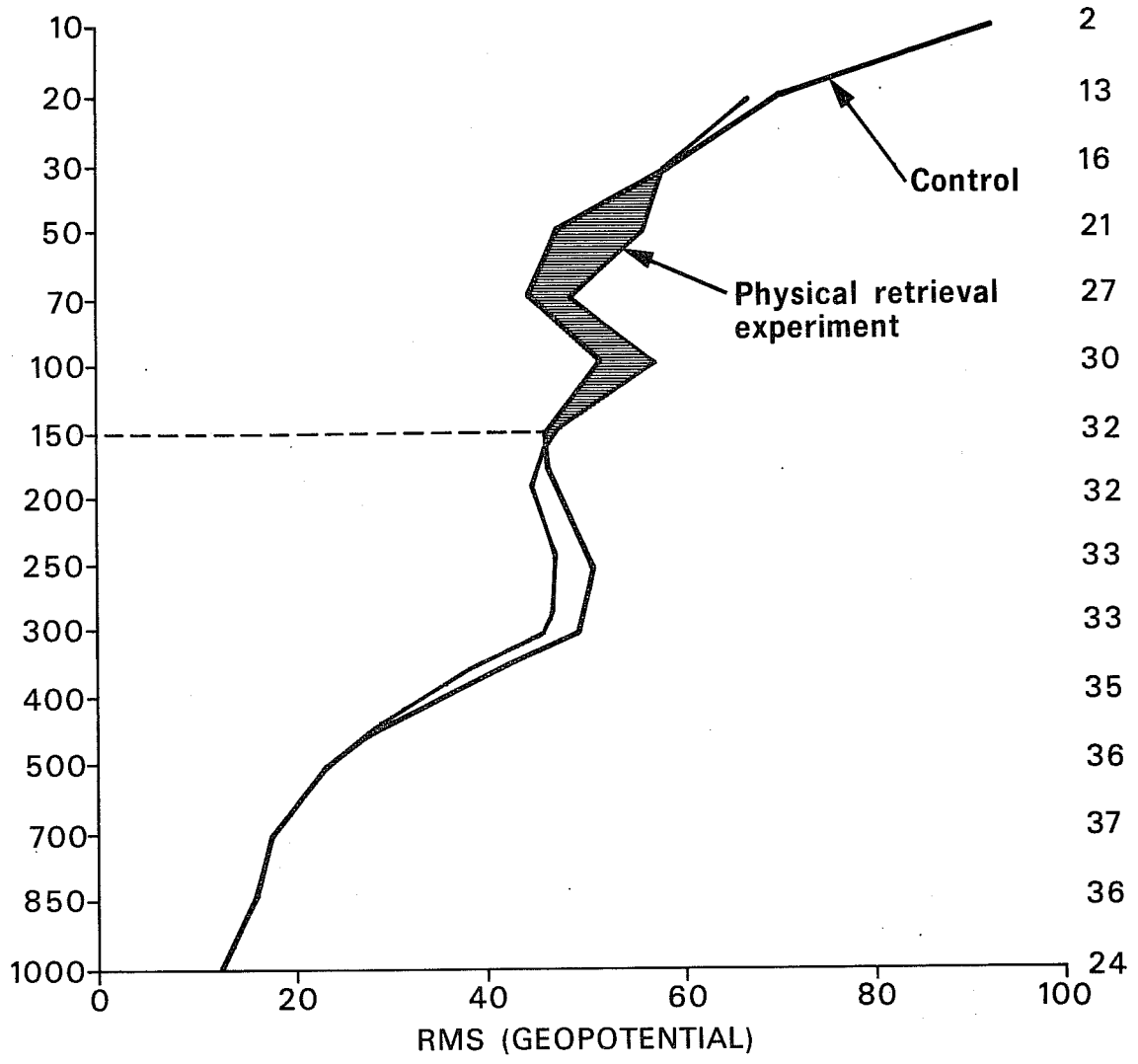

Fig. 9 rms fits of the first guess to the radiosonde geopotential height in the Southern Hemisphere, on 18 November 1979, 12Z.
Thin line: physical retrieval assimilation - Thick line: control.
Right column: number of data used in the computation.

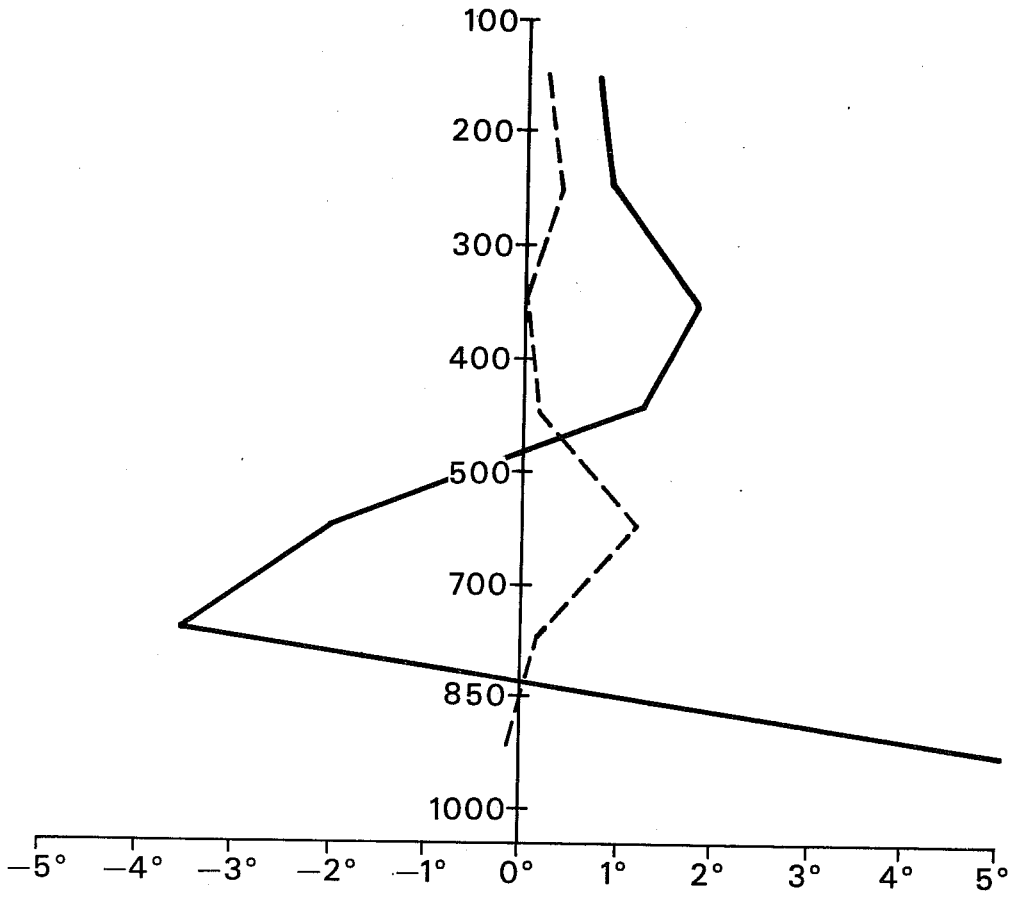

Fig. 12 Temperature differences between satellite soundings and the first guess on 18 November 1979 12Z, by 72N and 138W. Full line: statistical retrieval - first guess. Dotted line: physical retrieval - first guess.